Multi-objective Design and Optimization of Power Electronics Converters With Uncertainty Quantification—Part I: Parametric Uncertainty

Niloofar Rashidi, *Member, IEEE*, Qiong Wang, *Member, IEEE*, Rolando Burgos, *Member, IEEE*, Chris Roy, and Dushan Boroyevich, *Life Fellow, IEEE*

***Abstract*—This article presents a robust multi-objective design and optimization approach with parametric and model-form uncertainty quantification (MDO with P&MF-UQ). The first part of the article focuses on incorporating parametric uncertainty quantification (P-UQ) into the MDO framework, where a sensitivity index is defined as a quantitative measure of system design robustness with regards to manufacturing variability in the design of systems with multiple performance functions. To demonstrate the benefits of incorporating P-UQ analysis into the design optimization framework, this article presents the design and optimization of a robust high-efficiency high-power-density 1.25 kW Vienna-type rectifier. The optimum design solution is realized by exploring the Pareto Front of the enhanced performance space where the parametric sensitivity of each design point is considered to discern between cases and help identify the most parametrically-robust of the Pareto-optimal design solutions. It is shown that the design sensitivity is reduced by 39% when the optimum design is selected using MDO with P-UQ rather than the conventional MDO.**

***Index Terms*—Model-form uncertainty, multi-objective design optimization, parametric uncertainty (PU), robustness, sensitivity, tolerances, Vienna-type rectifier.**

I. Introduction

MULTI-OBJECTIVE design and optimization (MDO) approach in the field of power electronics was first developed within the framework of a road-mapping initiative that European Center for Power Electronics started in 2003 [2]; since then, this approach has been applied for the realization of ultracompact ultraefficient power converters [3]–[8].

Despite the inevitable tolerance associated with different system parameters, as well as variations in the operating conditions, uncertainties have not yet been considered in the presented computations within the MDO of power converters. As a result, their effect on the performance space and the resultant Pareto Front has been neglected. Whereas, the impact of these uncertainties on the predicted system performance measures, could potentially change the performance space and the resultant Pareto Front. In few cases, the effects of the component tolerance on system performance are investigated after selecting the final design; e.g., the particular combination of component values that lead to the worst-case condition is determined to ensure feasibility of the selected design in the presence of manufacturing variability [3].

Also, in the previous works discussing MDO, it is assumed that the mathematical models available for design optimization adequately model the system performance and make tradeoffs in interest for the problem. However, this assumption is, in principle, not valid because no model is perfect. Modeling inaccuracy introduces an additional source of variability in the design of power converters and systems [9]. Therefore, depending on the accuracy of the model for the selected design, actual performance of the converter could vary from the predicted performance ascertained using MDO approach.

In this article, a new method for MDO of power converters is proposed that accounts for the variations in system parameters and modeling errors when predicting the performance space and the resultant Pareto Front. This is achieved by incorporating parametric and model-form uncertainty quantification (P&MF UQ) into the MDO framework [10]. As a result, this approach includes robustness considerations with regards to manufacturing variability as well as modeling inaccuracies in the design of power converters with multiple performance functions. The first part of the article is dedicated to incorporating P-UQ into the MDO framework and it is organized as follows.

Section II provides a brief mathematical background of the MDO, in which the design process in general and the subsequent evaluation of the systems are first illustrated and shown in abstract form as the mathematical mapping of a design space into a system performance space. Following, the multi-objective optimization of this mapping is discussed. In Section III, the general system design flow is modified to incorporate P-UQ analysis into the design optimization framework. Section IV develops a new performance vector indicating design robustness.

Manuscript received January 26, 2020; revised April 28, 2020; accepted June 12, 2020. Date of publication July 15, 2020; date of current version September 22, 2020. This article was presented at 18th IEEE Workshop on Control and Modeling for Power Electronics, Stanford, CA, USA, July 2017. Recommended for publication by Associate Editor D. Xu. *(Corresponding author: Niloofar Rashidi.)*

Niloofar Rashidi, Qiong Wang, Rolando Burgos, and Dushan Boroyevich are with the Center for Power Electronics Systems, Bradley Department of Electrical and Computer Engineering, Virginia Tech, Blacksburg, VA 24061 USA (e-mail: rashidim@vt.edu; wangq@vt.edu; rburgos@ieee.org; dushan@vt.edu).

Chris Roy is with the Crofton Department of Aerospace and Ocean Engineering, Virginia Tech, Blacksburg, VA 24061 USA (e-mail: cjroy@vt.edu).

Color versions of one or more of the figures in this article are available online at https://ieeexplore.ieee.org.

Digital Object Identifier 10.1109/TPEL.2020.3005456

Furthermore, In Section V, the feasibility robustness is discussed, and the constraint functions are modified accordingly. Finally, Section VI demonstrates the benefits of incorporating P-UQ analysis into the MDO from a more practical standpoint; a thorough mathematical modeling and design optimization of a Vienna-type rectifier and its components, concerning efficiency and power density within given size limitations and operational requirements, are provided. MDO with built-in P-UQ is then used to design a robust free-convection cooled 1.25 kW Vienna-type rectifier. The final optimum design is realized by exploring the system Pareto Front of the enhanced performance space, where the parametric sensitivity of each design point is used to discern between cases and help identify the most parametrically-robust of the Pareto-optimal solutions. Finally, Section VII concludes the article.

II. Mathematical Formulation of Multi-objective Design Optimization

Circuit topology, modulation scheme, control parameters, magnetic core type, and core size are a few examples of the many design variables present in the design of power electronic systems and converters. Design variables are a group of system parameters in the design of power converters which are determined by designers. These variables are selected based on the available library and within given lower and upper bounds (for continuous variables) or from a limited number of options (for discrete variables). Each design variable is then assigned a coordinate axis forming an n-dimensional design space where n is the number of design variables.

Generally, in the design of power converters and systems, for each point in the design space, the behavioral model is run based on the given system specifications. All required information for the design of components, i.e., voltage and current waveforms, are extracted from simulation results, and appropriate passive and active devices, magnetic components, wires, etc., are selected accordingly. Besides design variables, the rest of the system parameters need to be determined such that side conditions defined by system specifications or minimum performance requirements are fulfilled. These parameters are called nondesign system parameters; they are not directly controlled by the designer and are a function of system specifications and design parameters. These parameters are realized through the system design flow for each design iteration to ensure system functionality and operational requirements.

According to the specified design criteria, required component models are also developed to predict the intended system behavior and selected performance measures. Performance measures (e.g., efficiency, size, cost, weight, etc.) are the indices that need to be maximized or minimized (depending on the MDO formulation) through a design process. These objectives are a function of design variables as well as nondesign system parameters. Each performance index is then assigned a coordinate axis forming an k-dimensional performance space where k is the number of performance indices.

By calculating all desired performance indices for a point in the design space through the general system design flow, the corresponding design can be represented with a point in the k-dimensional performance space. This procedure is iterated until all combinations of design variables (all the points in the design space) are swept with corresponding side conditions to ensure feasibility of the designs in the performance space.

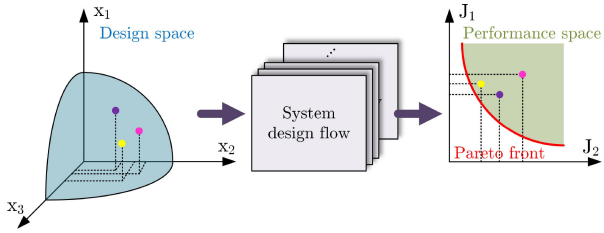

Fig. 1. Representation of the multi-objective design and optimization: mapping a multidimensional design space into a multidimensional performance space to determine the Pareto Front.

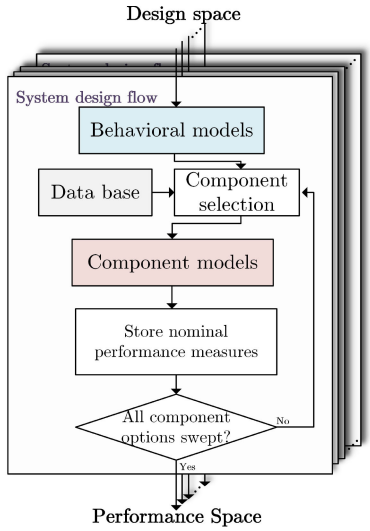

Fig. 2. Power electronics system design flow.

Hence, overall, the n-dimensional design space is mapped into the k-dimensional performance space (see Fig. 1). A general system design flow in the design of power converters is shown in Fig. 2, which includes a behavioral model of the power converter, component library, and component models. A switching model, for instance, is a behavioral model, as all information for selecting each component can be extracted from its simulation results. Loss and size models, on the other hand, are examples of component models, which are developed to predict the intended performance measures.

A typical mathematical formulation for mapping the design space into a performance space in the multi-objective design can be given as follows:

$$\mathbf{x} \rightarrow \mathbf{J}(\mathbf{x}, \mathbf{p}) \tag{1}$$

where $\mathbf{x}$ is the vector of design variables $(\mathbf{x} = [x_1, x_2, \ldots, x_n]))$, $\mathbf{p}$ is the vector of nondesign system parameters $(\mathbf{p} = [p_1, p_2, \ldots, p_m]))$, $\mathbf{J}$ is the vector of primary performance indices $(\mathbf{J} = [J_1, J_2, \ldots, J_k]))$, and n, m, and k are the number

of design variables, nondesign system parameters, and performance indices, respectively.

Within the scope of design optimization, the final step is to find the optimum design solution that maximizes the performance vector ($\mathbf{J}(\mathbf{x}, \mathbf{p})$) while satisfying constraints. A typical mathematical formulation of the MDO can be written as follows:

$$\max \mathbf{J}(\mathbf{x}, \mathbf{p}) \tag{2}$$

$$\text{such that (s.t.) } \mathbf{g}(\mathbf{x}, \mathbf{p}) \leq 0, \text{and}$$

$$\mathbf{h}(\mathbf{x}, \mathbf{p}) = 0 \tag{3}$$

$$\mathbf{x_{LB}} \leq \mathbf{x} \leq \mathbf{x_{UB}} \tag{4}$$

where $\mathbf{x}_{\mathrm{LB}}$ and $\mathbf{x}_{\mathrm{UB}}$ are the vector of lower and upper bounds for the vector of design variables, respectively. Functions $\mathbf{g}(.)$ and $\mathbf{h}(.)$ are side conditions describing the inner converter function, the system requirements or specifications, and minimum required values of other performance indices to ensure feasibility of the designs.

The optimum design solution is finally realized by exploring the Pareto Front that is the boundary of the feasible performance space. Many approaches have been studied to construct the Pareto Front [11]. Due to the limited number of objectives in this article, the weighted sum approach is used [12]. The weighted sum method assigns weights for each objective (performance function) based on the relative preferences among objectives and combines the multiple objectives into a single objective. The Pareto Front is then achieved by trying different weights for the individual objectives and performing the optimization multiple times. In other words, Pareto Front is realized using the following algorithm:

$$\sum_{i=1}^{k} w_i J_i(\mathbf{x}, \mathbf{p}) \rightarrow \mathrm{Max}; \quad \sum_{\mathrm{i}=1}^{\mathrm{k}} \mathrm{w_i} = 1 \tag{5}$$

where w_i is the weighting factor for the ith performance index. The maximum performance vector for all possible value combinations of weighting factors would be the resultant Pareto Front (shown in Fig. 1). Therefore, the MDO results in a set of Pareto-optimal solutions in the performance space. Considering a 2-D performance space, for any point on the Pareto Front, an increase in one performance index is only possible with a decrease in the other performance index. The final design point is ultimately selected from Pareto-optimal design solutions and is based on the compromise between individual optimization goals.

III. Modified System Design Flow

As described in the previous section, design optimization of a converter is generally done using the nominal values of all component parameters. However, in practice, there is a tolerance associated with different parameters of each component; these variations, also known as parametric uncertainty (PU), are mainly due to manufacturing variability. One of the approaches for solving MDO in the presence of PU is the probabilistic approach, where P-UQ is incorporated into the optimization formulation.

The uncertainty due to physical variability in the system properties and surrounding is often irreducible and is commonly represented by probability distributions. If an uncertain design variable or nondesign system parameter can be described using a combination of data points or an interval, then the principle of likelihood can be used to construct a probability distribution ($f_X(x)$). Assume the type of distribution (normal, lognormal, uniform, etc.) of x is known and let $\mathbf{L}$ denote the distribution parameters. Then, the probability density function (PDF) of x is denoted by $f_X(x|\mathbf{L})$. Note that this density function is conditional on the choice of parameters, and hence these parameters ($\mathbf{L}$) need to be estimated using the available evidence.

To account for PU, the system design flow must be modified accordingly, as the input parameters are no longer considered deterministic. As a result, optimization under PU requires an extra loop of computation, i.e., P-UQ, in each system design iteration where nondeterministic simulation is employed to propagate the uncertainties throughout the model to estimate the variability in the model outputs, such as performance indices and constraint functions. Therefore, at each design iteration, the output distributions and probabilities of satisfying constraint thresholds need to be evaluated given the design variable values.

As seen in Fig. 2, there are two types of models in the general system design process: behavioral model and component models. The governing differential equations of power electronics behavioral models rarely yield exact solutions for practical problems. Approximate numerical solutions must be used for this type of models. Component models, on the other hand, are usually analytical models and have a closed form solution. To reduce the computational effort for MDO with P-UQ, in the case of component models, for which the explicit solution to the model is available, the worst-case analysis is conducted to estimate the variability in the model output [13]. In the case of behavioral models, however, MC sampling must be used to propagate uncertainties throughout the model and estimate the variability in the model output [14]. Therefore, to incorporate P-UQ analysis, quasi-random MC simulation and worst-case analysis are incorporated into behavioral models and component models, respectively. Fig. 3 illustrates the flow diagram summarizing the system design process with built-in P-UQ.

IV. New Performance Vector

In the modified system design flow, multiple simulations must be conducted for each point in the design space. As a result, in each design iteration, instead of a single value for each performance measure, multiple values are generated to reflect the effect of manufacturing variability on the predicted performance indices. A PDF of uncertain performance measures can then be denoted by $f_J(j|\mathbf{L})$, which is conditioned on the choice of parameters; these parameters (mean, standard deviation, etc.) need to be estimated using the resultant data points from the nondeterministic simulation. Accordingly, for the design of a power converter to be optimized under PU, two goals must be formulated mathematically: first is maximizing the mean of

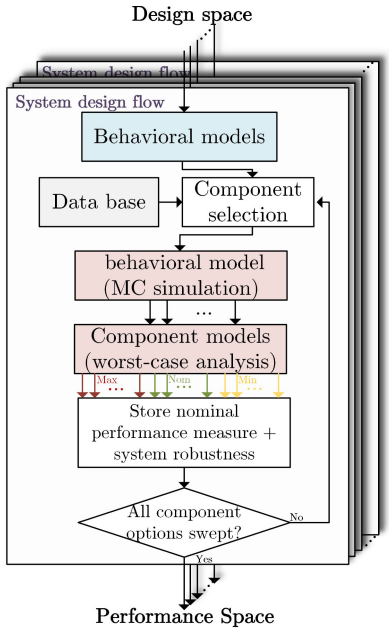

Fig. 3. Power electronics system design flow with built-in parametric uncertainty quantification (P-UQ).

the performance functions and the second is minimizing the variation of the performance functions, which is usually modeled by its variance or standard deviation. In other words, each performance function is now represented as two corresponding objectives in the MDO with P-UQ formulation.

These two objectives should be achieved simultaneously to ensure performance robustness and optimality. This will increase the set of objectives from k objectives to $2k$ as

$$\begin{aligned} &\max \mu_{\mathbf{J}}(\mathbf{x}, \mathbf{x_d}, \mathbf{p}, \mathbf{p_d}) \\ &\min \sigma^2_{\mathbf{J}}(\mathbf{x}, \mathbf{x_d}, \mathbf{p}, \mathbf{p_d}) \end{aligned} \tag{6}$$

$$\begin{aligned} &\mathbf{x_{dLB}} \leq \mathbf{x_d} \leq \mathbf{x_{dUB}} \\ &\mathbf{p_{dLB}} \leq \mathbf{p_d} \leq \mathbf{p_{dUB}} \\ &\mathbf{x_{LB}} + 3\sigma^2_{\mathbf{x}} \leq \ \mu_{\mathbf{x}} \leq \mathbf{x_{UB}} - 3\sigma^2_{\mathbf{x}} \\ &\mathbf{p_{LB}} + 3\sigma^2_{\mathbf{p}} \leq \ \mu_{\mathbf{p}} \leq \mathbf{p_{UB}} - 3\sigma^2_{\mathbf{p}}. \end{aligned} \tag{7}$$

In (6) and (7), $\mu_{\mathbf{J}}$ and $\sigma^2_{\mathbf{J}}$ are the mean and variance vectors of performance functions, rspectively, $\mathbf{x}_{\mathrm{dUB}}$, $\mathbf{x}_{\mathrm{dLB}}$, $\mathbf{x}_{\mathrm{UB}}$, and $\mathbf{x}_{\mathrm{LB}}$ are the vectors of upper and lower bounds on the deterministic and nondeterministic design parameters, respectively; $\mathbf{p}_{\mathrm{dUB}}$, $\mathbf{p}_{\mathrm{dLB}}$, $\mathbf{p}_{\mathrm{UB}}$, and $\mathbf{p}_{\mathrm{LB}}$ are the vectors of upper and lower bounds on the deterministic and nondeterministic nondesign system parameters, respectively; and $\mu_{\mathbf{x}}$, $\sigma^2_{\mathbf{x}}$, $\mu_{\mathbf{p}}$, and $\sigma^2_{\mathbf{p}}$are the mean and variance vectors of uncertain design and nondesign system parameters, respectively.

Since each performance function is represented as two objectives, the MDO formulation can quickly become intractable even with a small number of objectives. In addition, a large number of objective functions in such problems cause an inability to graphically visualize the Pareto set to understand tradeoffs introduced by design robustness considerations. Thus, the main drawback of such methods is that they become burdensome to solve as the number of performance functions increases [15]–[18]. A new approach has been proposed in [19] that tackles both robustness and optimality using the joint PDF of all the performance functions. The MDO problem is hence reduced to a 2-D optimization problem regardless of the number of objectives. However, this approach cannot be readily visualized and interpreted; such a representation lacks any information regarding the tradeoffs between different performance measures, whereas this information is typically expected to aid in decision-making for MDO problems.

In the formulation proposed in this article, the sensitivity index is first defined for the performance function to provide a measure of robustness for each primary performance index in the presence of PU. The aggregated function of individual sensitivity indices, herein after referred to as total sensitivity, is then used as an additional performance measure in the MDO formulation. This new performance measure represents the total sensitivity of the design with regards to PU. Such a representation takes into account the manufacturing variability in the decision-making by minimizing a scalar quantity irrespective of the number of performance functions.

In this article, the following formula is used to calculate the sensitivity index for each performance measure

$$S_i = \frac{3\sigma_{j_i}(\mathbf{x}, \mathbf{x_d}, \mathbf{p}, \mathbf{p_d}))}{\mu_{j_i}(\mathbf{x}, \mathbf{x_d}, \mathbf{p}, \mathbf{p_d}))} \tag{8}$$

where σ_{j_i} and μ_{j_i} are the standard deviation and mean value of the ith performance index, respectively, and S_i is the resultant sensitivity index of the ith performance measure. As shown in (8), to calculate sensitivity indices, the tolerance of each performance index is normalized with respect to its mean value to avoid scaling issues when aggregating the sensitivity indices; this can occur when the variances of the performance functions are of largely disparate magnitudes.

The individual sensitivity indices are finally aggregated using weight-based methods by expressing preferences between objectives using weights; this results in a total sensitivity index for each design point. The weightings of the individual performance indices determine the compromise between the individual optimization goals. The total sensitivity index (S_T) is hence calculated based on the compromise between individual performance measures according to the optimization goals as

$$S_T = \sum_{i=1}^{k} w_i S_i; \quad \sum_{i=1}^{k} w_i = 1. \tag{9}$$

The new performance vector is finally expressed as

$$\begin{aligned} &\max \mu_{\mathbf{J}}(\mathbf{x}, \mathbf{x_d}, \mathbf{p}, \mathbf{p_d}) \\ &\min S_T. \end{aligned} \tag{10}$$

In the proposed MDO formulation, the final performance space will have an additional performance index, which is the total sensitivity. As shown in Fig. 4, in the new performance space, the tradeoffs can be easily visualized using the aggregated sensitivity index of the performance functions. As the total sensitivity of a design approaches zero, the design would be

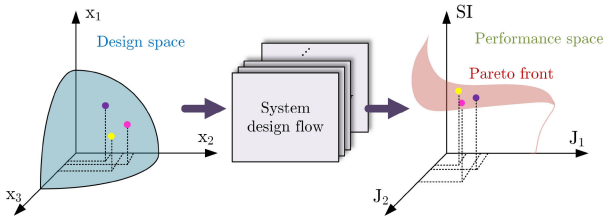

Fig. 4. Representation of the multi-objective design and optimization with uncertainty quantification (MDO with UQ): mapping a multidimensional design space into an enhanced multidimensional performance space with sensitivity index to determine the Pareto Front.

more robust in the presence of manufacturing variability. An alternative design with a lower sensitivity index should hence be selected as the final optimum design. Consequently, total sensitivity can potentially be used as a measure of system design robustness to evaluate performance trends in the field of power electronics.

V. MDO With Built-in P-UQ

The previous section described how MDO with design robustness considerations could be accomplished by adding a P-UQ loop in the system design flow and modifying the performance vector accordingly. In this article, however, besides performance robustness, feasibility robustness is also considered; this is concerned with ensuring that the constraints are adequately fulfilled under uncertainty. Similar to performance objectives, as a result of incorporating UQ analysis, the constraint functions in the new MDO formulation are also modified to account for the effects of PU as

$$\begin{aligned} \text{s.t.}\quad & \text{Prob}(\mathbf{g}(\mathbf{x}, \mathbf{x_d}, \mathbf{p}, \mathbf{p_d}) \leq 0) \geq P_{\text{target}}, \quad \text{and} \\ & \text{Prob}(\mathbf{h}(\mathbf{x}, \mathbf{x_d}, \mathbf{p}, \mathbf{p_d}) = 0) \geq P_{\text{target}} \end{aligned} \tag{11}$$

where P_{target} is determined based on the intended level of confidence. For instance, if $P_{\text{target}} = 100\%$ is selected then the constraints should be satisfied under the entire range of the resultant distribution, setting a more stringent requirement for the optimization.

Even though the operating conditions are subject to variability such as load and source variation, and changes in the temperature, S_T has been calculated for the nominal operating conditions. However, to ensure feasibility of the design under uncertainty in practice and for a design point to be included in the final performance space, the design should satisfy the constraints under the worst-case condition. MDO constraints are therefore modified as

$$\begin{aligned} \text{s.t.}\quad & \text{Prob}(\mathbf{g}(\mathbf{s}_{\text{wc}}, \mathbf{x}, \mathbf{x_d}, \mathbf{p}, \mathbf{p_d}) \leq 0) \geq P_{\text{target}}, \quad \text{and} \\ & \text{Prob}(\mathbf{h}(\mathbf{s}_{\text{wc}}, \mathbf{x}, \mathbf{x_d}, \mathbf{p}, \mathbf{p_d}) = 0) \geq P_{\text{target}} \end{aligned} \tag{12}$$

where $\mathbf{s}_{\text{wc}}$ is the vector of variables defining the worst case operating conditions.

VI. Case Study: Design Optimization of a Vienna-Type Rectifier

In the development of power electronics systems for More Electric Aircraft (MEA) [20], [21], the power density and efficiency have been a primary concern [22], [6]. The Pareto Front concept has thus been carried out in the MDO of these power converters to realize the performance limit based on the available degrees of freedom and to ultimately determine the optimum design [2]. The main contribution of this section is to present the benefits of incorporating UQ analysis into the MDO from a more practical standpoint. For illustrative purposes, the Vienna-type rectifier, a popular topology for implementing ac–dc mains interface in MEA, is used as a case study to compare the theoretical analysis with a comprehensive experimental validation. First part of this article is focused on benefits of P-UQ, the MF-UQ will be discussed in the second part of this article.

A. System Specifications and Requirements

The power electronics supply of high-power systems from the three-phase ac mains in MEA applications is usually carried out in two stages: The mains ac voltage is first converted into a dc voltage, which is then adapted to the load voltage by a dc–dc converter with galvanic isolation [21], [23]. This article focuses on design optimization of the ac–dc converter in the first stage.

In modern aircraft power systems, three-phase active pulsewidth modulation (PWM) rectifiers are well suited for implementing ac–dc power converters, as they feature superior performance in comparison with other topology candidates in terms of efficiency, input-current quality, and weight [7]. In this article, a Vienna-type rectifier is selected as the targeted topology for implementing the active front end (AFE) rectifier due to its high efficiency as compared with other topology candidates; this will be further discussed later in this section.

The primary objective of this article is to optimize the design of a local converter card with regards to design robustness, efficiency, and power density, while addressing combined power quality, EMI, and thermal requirements. An aircraft variable frequency ac power bus feeds the converter and output power should provide 345 V dc voltage. The converter will be designed for the maximum tenable power rating within the given constraints of volume $(8.3 \times 7.26 \times 1\ \text{in}^3)$ and total loss (30 W) under specified operating conditions. To avoid any active cooling in the converter, an efficiency of greater than 98% is required. Given the minimum required efficiency to achieve free-convection-cooled design and the required margin for allocated loss in the worst-case condition, the maximum attainable power rating of the converter is set to approximately 1.25 kW. The system specifications and operating conditions of the converter are summarized in Table I.

In summary, according to MDO objectives, the primary performance indices in this article are loss and size of the converter. The final converter should also comply with the DO-160 standard for EMI and power quality. These specifications set the limitations in the converter design optimization, as described in the next section.

TABLE I
SUMMARY OF SYSTEM SPECIFICATIONS

Parameter	Nominal Value
Nominal output power, P_{out}	1.25 kW
Line-to-line rms input voltage, V_{ac}	115 V $\pm$ 10%
Nominal output dc voltage, V_o	345 V
Line frequency, f_o	360 Hz ~ 800 Hz
Operation temperature, T_a	-40 °C ~ 70 °C

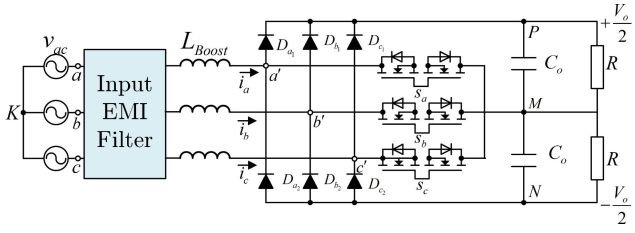

Fig. 5. Circuit schematic of the Vienna-type rectifier.

B. Converter Design Considerations

Design of a converter is comprised of several steps, including topology selection, input/output filter design, modulation implementation, implementation of passive components, selection of semiconductor devices, and design of the control system; each of these steps is discussed in the following sections, in which key design variables are identified and described.

1) Topology Selection: Although conventional two-level boost rectifiers have become dominant in the industry, if higher efficiency is required, three-level converters present a better solution. The most renowned three-level implementation of a three-phase active PWM rectifier is the Vienna-type rectifier. The main advantage of this topology is its high reliability due to the impossibility of shoot-through failure modes. Although the forward-voltage drops of the diodes in this rectifier result in high conduction losses, the development of SiC Schottky diodes with high blocking voltage and, ideally, no reverse-recovery current has eliminated this source of loss and has further improved the efficiency of this converter [24].

The circuit schematic of the selected topology is shown in Fig. 5, in which a Vienna-type rectifier converts three-phase variable-frequency ac input voltage into regulated dc voltage while providing the PFC function. Among various phase-leg configurations, the one used in this article features the highest efficiency [24]. For active switches, Vienna-type rectifiers require four-quadrant switches to block voltage and conduct current in both directions. Two MOSFETs are hence connected in a common source configuration in this topology. There is also an input EMI filter added to the three-phase converter to make the converter comply with EMI and power-quality standards; this will be further discussed later in this article.

2) Modulation Scheme: Although it is shown that discontinuous pulsewidth modulation (DPWM) to be the best modulation scheme in achieving the highest efficiency [25], it lacks the flexibility of choosing a redundant vector, which will result in poorer harmonic performance compared to continuous pulsewidth modulation (CPWM). This situation is even more significant at lower modulation-index values, and results in a dominant third harmonic in the neutral-point current. This current flows into the parallel connection of the output capacitors, and the implementation of neutral-point voltage control may introduce further switching transitions. Therefore, to maintain the same level of third-harmonic voltage ripple as in CPWM, an increase of output capacitance value is required; this, in effect, results in a reduction in power density. Although requirements such as the hold-up time may dominate over the mentioned increase in the dc capacitor, given the design requirements in this article, CPWM is selected as the modulation scheme to achieve a higher power density design.

In CPWM, the ripple of the phase current in the mains is influenced by the distribution of redundant switching states. In the development of space-vector PWM, the zero space vector positions are left undefined and there is an opportunity to explore possible harmonic benefits by manipulating the placement of zero pulses [26]. In this article, center-aligned SVM is used; the active space-vector is centered in each half-carrier period and the remaining zero space-vector time is split equally, such that the redundant vector occurs at the first and last positions of the switching sequence. This will essentially improve the input-current quality to better comply with power quality standards.

3) Switching Frequency: A relatively high switching frequency is required to obtain a low design volume of magnetic components to further increase the power density in the design of power electronic systems. However, high switching frequency results in an increase in frequency-dependent losses (e.g., switching loss, skin and proximity effect loss, etc.), and hence a relatively lower efficiency design will be achieved. As a result, if the switching frequency is increased above a certain limit, the volume of the cooling system finally dominates, and the output-power density will be reduced. Thus, to maintain an efficiency of higher than 98% to avoid any active cooling, and according to preliminary calculations, the maximum switching frequency in this design is limited to 92 kHz.

Minimum switching frequency, on the other hand, is determined according to the DO-160 power quality standard. This power quality standard has limitations up to 40th-order harmonics; given the frequency range for the mains (360 $\sim$ 800 Hz), this would limit the minimum switching frequency to values higher than 32 kHz.

4) Boost Inductance: The boost inductance will affect low-frequency current harmonics, which are critical to meeting the power quality standard. For the selected boost-inductance value, therefore, the power quality must be checked to ensure compliance with the standard. The boost-inductance value must also increase with the reciprocal of the switching frequency to retain a relatively low switching frequency ripple in the input current. Given the maximum and minimum allowable switching frequencies in this design, the final range for boost-inductance value in this design is 210 $\sim$ 450 μH.

5) DM EMI Filter: A *CLCL* structure has been selected as the differential mode (DM) EMI filter configuration per phase [7]. In this configuration, a damping resistor is also added in series with the DM capacitor to damp unwanted current noise

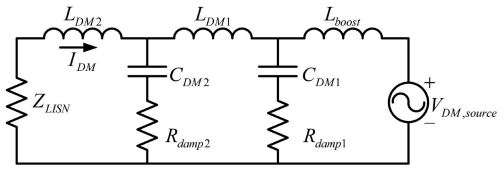

Fig. 6. Converter differential mode model.

in the power-quality standard band (up to 32 kHz) that is caused by filter resonance.

The DM filter capacitance value is selected based on the reactive power constraint and rectifier functionality described in the following. For a Vienna-type rectifier, the angle between phase-leg current and voltage should be low enough to ensure correct modulation; this requirement places limitations on the total allowed filter capacitance. The angle limit ($\theta_{\lim}$) is given by (13)

$$\theta_{\lim} = \left|\arcsin\left(\frac{1}{\sqrt{3}M} - \frac{\pi}{6}\right)\right| = 0.124 \text{ rad} \tag{13}$$

where M is the modulation index and is defined as $2V_{ac,pk}/V_o$. Assuming unity power factor is achieved at the input terminals, this limits the angle between the filter's reactive power and the converter's active power, as follows:

$$\arcsin\left(\frac{Q_f}{P_o}\right) < \theta_{\lim} \tag{14}$$

$$\arcsin\left(\frac{|Q_f|}{P_o}\right) \approx \arcsin\left(\frac{\left|2\pi f_{\text{in}} L_f I_{\text{in,rms}}^2 - 2\pi f_{\text{in}} C_f V_{\text{in,rms}}^2\right|}{I_{\text{in,rms}} V_{\text{in,rms}}}\right) \tag{15}$$

where L_f is the total inductance and C_f is the total capacitance per phase. Based on (15), the total allowed filter capacitance is related to the input frequency, active power, and total filter inductance. However, the second term in (15) is dominant in determining the phase angle between the filter's reactive power and the converter's active power. Therefore, changes in the total inductance value will not significantly affect this angle. In this design, the minimum required capacitance is estimated such that the correct modulation is guaranteed under half load with 800 Hz input frequency. The minimum required C_{DM} is estimated to be 0.22 μF and the 0.22 μF EPCOS MKT film capacitor is selected.

The minimum required DM filter inductance is then calculated based on EMI constraints as follows. For a given operating condition, the output-voltage spectrum of each phase leg (referred to as $v_{a'}$, $v_{b'}$ and $v_{c'}$) can be calculated using the Matlab Simulink simulation model or analytical models, i.e., by applying double Fourier transformation to the modulator reference and carrier. A limited range of possible damping resistor values is defined accordingly to ensure that the design complies with the power quality standard. With the voltage spectrum calculated, and the filter capacitance and damping resistance selected, DM inductance can be derived based on the EMI standards using the DM model (shown in Fig. 6), in which DM source voltage magnitude is calculated as

$$V_{DM,\text{source}} = v_{a'} - \frac{v_{a'} + v_{b'} + v_{c'}}{3}. \tag{16}$$

6) DC Output Capacitance: The dc bus capacitance value (C_o in Fig. 5) is determined by the output power. This capacitor is also selected such that the voltage rise on the dc bus capacitors at sudden load will not exceed the voltage limit of either the capacitor or the semiconductor devices. Also, for overall power density, the design volume of the output capacitor is considered.

Furthermore, as discussed earlier, the neutral voltage ripple is influenced by input frequency and the modulation index. Depending on the selected modulation scheme, third-order harmonics can be found on neutral-point voltage, which will result in $(6k+1)$th-order harmonics in input current, where $k \in \{1, 2, \ldots\}$. As such, for a Vienna-type rectifier, which is a three-level converter, the low-frequency ripple on the two dc bus capacitors, which is known as the neutral-point ripple, may influence the input-power quality. As a result, the dc bus capacitance should be large enough to ensure compliance with the power quality standard. In this design, 15 μF EPCOS MKP film capacitors are selected.

7) Magnetic Cores: A core material and core geometry must be selected for magnetic components, i.e., the DM and boost inductors. In this article, for boost and DM filtering inductor implementation, Ferroxcube 3C95 ferrite cores (effective volume: 5470 $\sim$ 52600 mm^3), and Magnetics Inc. MPP iron-powder cores (effective volume: 960 $\sim$ 10600 mm^3) are considered. It should be noted that the other aspects of the inductor design, such as realization of air gap length, number of turns, winding arrangements, winding cross-section or copper foil, etc., are specified later as nondesign system parameters through the system design flow.

8) Semiconductor Devices: The total loss in a Vienna-type rectifier is dominated by the conduction and switching losses of the power semiconductors. Hence, at a given switching frequency, a possibility of maximizing the efficiency appears through the optimum choice of power semiconductor devices.

MOSFETs with lower ON-resistance have higher junction capacitance, which result in higher switching losses. The ON-resistance of the MOSFETs is therefore a critical parameter in determining loss and is used as a design variable to select device candidates. In this article, 250 V Si MOSFETs with 20 and 60 mΩ ON-resistance from Infineon are selected (IPB200N25N G3 and IPB600N25N G3).

The loss generated by diodes is not limited to conduction loss, as they will also generate switching losses due to charging and discharging of their junction capacitors. To achieve maximum efficiency, diodes should be carefully selected with consideration given to their influence on both conduction loss and switching loss. Diodes with larger current capability have higher junction capacitance values that generate more loss. Therefore, current capability is used as a design variable to select diode candidates. In this article, 650 V SiC Schottky diodes with 16 and 20 A current rating from CREE are selected (IDH20G65C5 and IDH16G65C5).

C) Multi-objective Design Optimization

1) Design Variables: In this section, a sweeping program is executed to find all possible value combinations of system-design variables to determine the final design space. It is worth noting that although certain design variables, such as AFE topology, EMI filter structure, modulation scheme, and control parameters, have been predetermined based on previous studies, any of these variables could have been realized through an MDO process with the penalty of higher computational cost.

The design procedure described in this article is based on the systematic approach for designing the ac–dc converter presented in a previous work [6]. This procedure starts with the definition of converter specifications and standards. Following, the switching-frequency and boost-inductance values are selected from the available range, after which the voltage spectrum can be derived from switching-model simulation results using the center-aligned SVM modulation scheme. Damping resistance is then selected from the available options. The minimum required DM inductance of the converter is then calculated as described earlier in this article.

At the end of each iteration, power quality requirements are checked for up to the 40th harmonic of the input current as well as EMI requirements for 150 kHz up to 10 MHz. If both standards are met, then the values of the design variables are stored. In the preliminary design process, only the system design parameters are swept. Semiconductors, core size, and core type are component-level design variables, which are added to the final design vector. This would result in a 9-D design space comprised of the following design variables: MOSFET on resistance, diode current rating, switching frequency, DM inductor-core type, DM inductor-core size, boost inductance value, boost inductor-core type, boost inductor-core size, and damping resistance value. It is worth noting that the rest of nondesign system parameters, such as the number of turns and air gap length for DM and boost inductors, are calculated separately for each design point to complete the design process of the converter.

2) Performance Indices: According to the primary goal of the optimization process, loss and size of the power converter need to be calculated at each design point. The required models for calculating loss and size have thus been implemented in the system-design flow as described in the following. It should be noted that the circuit operation information required by loss and size calculation models (e.g., current through devices, flux density change in inductor cores, etc.) is captured by the switching model of a Vienna-type rectifier, which is implemented in MATLAB Simulink.

The losses in a Vienna-type rectifier result mainly from its semiconductor devices and inductors. In this work, corresponding models for the conduction and switching losses of semiconductor devices, as well as the magnetic core and winding losses of inductors, have been developed and implemented in the system design flow as discussed in [27]–[29]. Notably auxiliary circuits, including DSPs, provide a fixed amount of loss that is not dependent on the operating point of output power, and thus these circuits are not included in the loss model for MDO.

Many of the parameters used in loss models are temperature dependent. On the other hand, thermal considerations are one of the constraints in the MDO of the Vienna-type rectifier. As a result, estimating the temperature rise of a component is required and thermal models have been implemented, mainly for those components that contribute significantly to the total loss of the converter (e.g., diode, MOSFET, and boost inductor). Consequently, an accurate estimate of model input parameters is provided while ensuring that the temperature of a component is not exceeding its maximum limit.

According to size constraints defined earlier in this section, the height of all components is limited to 1 in. Also, it is assumed that no inductors, capacitors, or semiconductor devices are placed over other devices. The total space occupied by each device is hence calculated by the multiplication of its footprint area and the height limit. Thus, in this optimization, the footprint area is taken as the performance index representing the size of the converter.

The dimension for each component is extracted from the available library, and the footprint area is calculated accordingly. The footprint area of the final converter is the sum of the calculated footprint areas for all components. Whereas in the final prototype, there will be free spaces between components due to the minimum required clearance distance, smooth air flow, and nonoptimum placements of the components. As a result, the size of the realized hardware is expected to be greater than the estimated value based on the component size models. This increase in the final converter size is assumed to grow linearly as the footprint area increases; and hence footprint area is considered as a fair index for comparing size of the designs.

3) Conventional MDO: In this section, the design of a Vienna-type rectifier is represented as a mathematical mapping of the design space derived earlier in this article into the performance space using the developed models.

To this end, through the conventional system-design flow for each point in the multidimensional design space, the switching model of the Vienna-type rectifier is run using the parameter values corresponding to the selected design point. The required information for selecting system components, such as operation parameters (e.g., rms/average current flowing through components), and component values (e.g., boost inductance, DM inductance, and damping resistance), with constraints of system operational requirements (temperature, EMI standard, and power quality standard) is extracted from simulation results of the behavioral model. All active and passive components are then designed and optimized based on the values given by the selected point in the design space, behavioral simulation results, and commercially available components. Loss and size models are then used to calculate values of performance indices of each design.

At the end of the optimization procedure, total loss and size are calculated at each design point, mapping the multi-dimensional design space into the 2-D performance space. Fig. 7 shows the resultant feasible performance space derived from the MDO of the 1.25 kW Vienna-type rectifier using the information from the database, switching model of the converter, and component models.

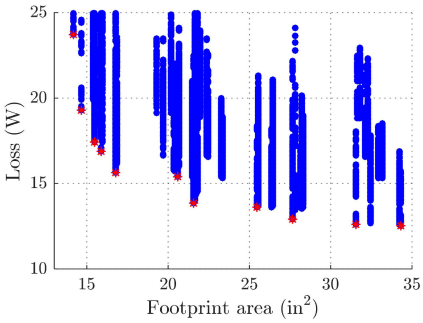

Fig. 7. Performance space of the Vienna-type rectifier indicating loss-size Pareto Front at 1.25 kW rated power; Pareto-optimal design solutions are indicated by red stars.

The main benefit of projecting many converter designs into the multidimensional performance space is that it makes an easier comparison of the trade-off between multiple performance indices and allows for clear decision making. As shown in Fig. 7, the Pareto Front of the Vienna-type rectifier is then determined (indicated by the red stars). For the design points on the Pareto Front, a decrease in the loss is only possible with an increase in the size, and no design exists that would offer the same size with a lower loss.

The final design point is ultimately selected based on the compromise between individual optimization goals; the selected Pareto-optimal design point based on the conventional MDO (MDO without UQ) features 21.58 in^2 total footprint area and 14.02 W loss. It should be noted that there are tens of other Pareto-optimal design points available with predicted performances quite similar to the selected design. In the next section, an enhanced performance space with the sensitivity index is used to discern between cases and to help identify the design that is the most parametrically robust among the Pareto-optimal solutions. Further, the feasibility of the design at the worst-case condition is checked as an additional MDO constraint.

4) MDO With P-UQ: The switching model of the Vienna-type rectifier, as a behavioral model, is used to predict the behavior of a power converter to extract the required information for design and optimization of all active and passive components. Loss and size models, on the other hand, as component models are used to predict performance measures. Therefore, to incorporate P-UQ analysis, a quasi-random MC simulation and WC analysis are incorporated into the switching model of the Vienna-type rectifier and loss/size models of components, respectively.

Through the system design flow with P-UQ (see Fig. 3), for each point in the multidimensional design space, the switching model of the Vienna-type rectifier is run using the parameter values corresponding to the selected design point. Similar to the conventional approach, key design variables of the Vienna-type rectifier are identified and swept. With design variables selected, values of passive components are calculated based on simulation and analytical models to address EMI and power quality requirements.

Also, in the modified system design flow, in addition to the nominal value for a nondeterministic parameter, its associated tolerance is also required. To predict primary performance measures in the system design flow with P-UQ, multiple simulations must be conducted for each point in the design space. According to the number of uncertain parameters in the conducted MC simulation and the target confidence interval, in this article, the minimum required resolution for the MC output is set to 500 data points that are then used in worst-case analysis to estimate mean, upper, and lower boundaries for each performance measure.

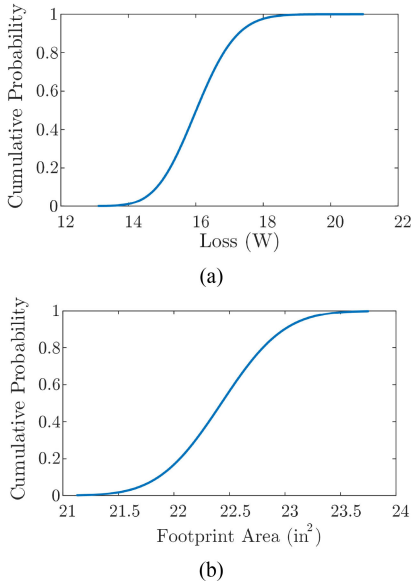

Fig. 8. CDF of the fitted distribution for: (a) loss and (b) size (footprint area) of a design based on MC and WC analyses.

The estimated upper, lower, and mean distributions are then used to estimate the required parameters ($\mathbf{L}$) for defining a PDF ($f_J(j|\mathbf{L})$) for each performance measure. Based on the estimated parameters in this article, the resultant estimated loss and size values corresponding to each design point have lognormal and normal distributions (see Fig. 8) with an associated PDF derived as (16) and (17), respectively

$$J_1 \sim Log\text{normal}\left(e^{\left(\mu_{J_1}+\frac{\sigma_{J_1}^2}{2}\right)}, e^{\left(2\mu_{J_1}+\sigma_{J_1}^2\right)}\left(e^{\sigma_{J_1}^2}-1\right)\right) \tag{17}$$

$$J_2 \sim \text{Normal}\left(\mu_{J_2}, \sigma_{J_2}^2\right) \tag{18}$$

where J_1 and J_2 are loss and footprint area, respectively. The sensitivity index for each performance measure is then calculated based on the derived distribution of each performance index using (8). The total sensitivity index is ultimately calculated using (9), where $w_1 = 0.9$ and $w_2 = 0.1$ are weighting factors for loss and size, respectively. The total sensitivity index is hence calculated based on the compromise between the sensitivity of loss and size with regards to manufacturing variability and it is utilized to help identify the most robust Pareto-optimal design solution. The total sensitivity in this approach is an aggregated measure of robustness for performance indices. Therefore, minimizing the total sensitivity results in minimization of loss and

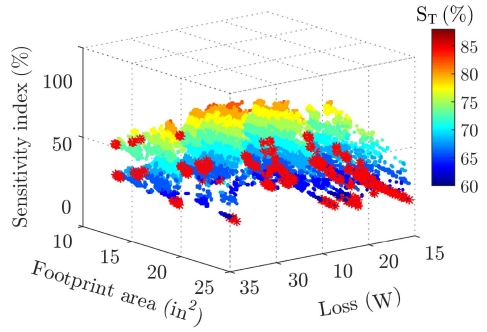

Fig. 9. Enhanced performance space of the Vienna-type rectifier indicating loss-size-sensitivity Pareto Front under 1.25 kW rated power. Pareto-optimal design solutions are indicated by red stars.

size variations individually, while favoring loss due its higher weighting factor.

Although, the total sensitivity of a design is calculated under nominal operating conditions (25 °C ambient temperature, 115 V ac voltage, and 100 Ω resistive load), to ensure the feasibility of the designs realized in the performance space the constraints must be fulfilled under the worst-case condition; that is 70 °C ambient temperature, 100 V ac voltage, and 95 Ω resistive load.

In the end, a high-density performance space is mapped from the design space to a 3-D performance space. Fig. 9 illustrates the enhanced performance space resulting from MDO with P-UQ, with the total sensitivity as the third performance index. The parametric sensitivity of each design point provides a comprehensive design criterion to enable the selection of the most robust Pareto-optimal solution. Therefore, an alternative design with lower total sensitivity index should be selected as the final optimum design. Additionally, as a result of modifying the constraints and adding a third performance measure in MDO with P-UQ, there is 32% reduction in the number of feasible design points and 2200% increase in the number of Pareto-optimal solutions in the performance space shown in Fig. 9 as compared to the 2-D performance space shown in Fig. 7. The total sensitivity index of the design points shown in Fig. 9 ranges from 17.3% to 74%; this range is limited to 17.3%–50% for the Pareto-optimal solutions.

The total sensitivity of the preselected optimum design based on the conventional MDO approach is 49.7%, i.e., the estimated loss using the exact parameters of 95% of the hardware units built based on this design ranges from 8.97 W to 22.90 W.

As a result of including P-UQ in the MDO, alternative designs with quite similar primary performance measures but relatively lower sensitivity compared to the preselected optimum design are realized in the performance space. Finally, the most robust Pareto-optimal design with 30.6% parametric sensitivity, 21.58 in^2 total footprint area, and 14.10 W loss is selected. According to the estimated loss and sensitivity index, 95% of the converters built based on this design would have a loss within 11.29 and 20.00 W.

As seen, the converters built based on the selected robust Pareto-optimal design are expected to have the least variability in their performance measures (e.g., less variability in the measured loss and size) and the best overall performance compared with the ones built based on the rest of the Pareto-optimal design solutions. It should be noted that this conclusion cannot be fully trusted, as its validity relies on the accuracy of modeling and simulation results, which have not yet been considered. This realization will be addressed in the second part of this article where MFU is included in the MDO framework to validate the models used in the MDO framework [30].

VII. Conclusion

In this article, a new design optimization approach was proposed to quantify and formulate design robustness with regards to manufacturing variability in the design problems with multiple performance functions. In this approach, the total sensitivity was introduced as a new performance measure. This scalar value represents robustness of the primary performance objectives. To this end, a modified system design flow was illustrated to integrate P-UQ analysis into the MDO. Regardless of the number of performance objectives considered, the proposed formulation results in an additional performance index, while ensuring that design robustness considerations are addressed jointly for all objectives, and that constraints are adequately fulfilled under uncertainty.

MDO with P-UQ was then applied to the design optimization of a 1.25 kW Vienna-type rectifier, with regards to its primary performance measures, i.e., loss and size, and the total sensitivity, while considering specific design constraints and operation requirements. The final optimum design was realized by exploring the system loss-size-sensitivity Pareto Front of the enhanced performance space where the parametric sensitivity of each design point was used to discern between cases and to help identify the most parametrically robust of the Pareto-optimal solutions. It was shown that the design sensitivity is reduced by 39% when the optimum design is selected using MDO with P-UQ rather than the conventional MDO.

Acknowledgment

The authors would like to thank Dr. Vladimir Blasko, Senior Fellow, Power Electronics, at United Technologies Research Center, for the generous support granted through a power electronics fellowship at Virginia Tech.

References

[1] N. Rashidi Mehrabadi, Q. Wang, R. Burgos, and D. Boroyevich, "Multi-objective design and optimization of a Vienna rectifier with parametric uncertainty quantification," in *Proc. IEEE 18th Workshop Control Model. Power Electron.*, 2017, pp. 1–6.

[2] J. W. Kolar, J. Biela, S. Waffler, T. Friedli, and U. Badstübner, "Performance trends and limitations of power electronic systems," in *Proc. 6th Int. Conf. Integr. Power Electron. Syst.*, 2010, pp. 1–20.

[3] D. O. Boillat, F. Krismer, and J. W. Kolar, "Design space analysis and $\rho - \eta$ pareto optimization of *LC* output filters for switch-mode AC power sources," *IEEE Trans. Power Electron.*, vol. 30, no. 12, pp. 6906–6923, Dec. 2015.

[4] J. W. Kolar, J. Biela, and J. Minibock, "Exploring the pareto front of multi-objective single-phase PFC rectifier design optimization-99.2% efficiency vs. 7kW/din 3 power density," in *Proc. IEEE 6th Int. Power Electron. Motion Control Conf.*, 2009, pp. 1–21.

[5] K. Raggl, T. Nussbaumer, G. Doerig, J. Biela, and J. W. Kolar, "Comprehensive design and optimization of a high-power-density single-phase boost PFC," *IEEE Trans. Ind. Electron.*, vol. 56, no. 7, pp. 2574–2587, Jul. 2009.
[6] Q. Wang, R. Burgos, X. Zhang, D. Boroyevich, A. White, and M. Kheraluwala, Optim. Des. Procedure Active Power Converters Aircr. Elect. Power Syst., SAE Tech. Paper No. 2016-01-1989, 2016.
[7] Q. Wang, X. Zhang, R. Burgos, D. Boroyevich, A. White, and M. Kheraluwala, "Design and optimization of a high performance isolated three phase AC/DC converter," in *Proc. Energy Convers. Congr. Expo.*, 2016, pp. 1–10.
[8] Q. Wang, X. Zhang, R. Burgos, D. Boroyevich, A. White, and M. Kheraluwala, "Design and implementation of a two-channel interleaved Vienna-type rectifier with >99% efficiency," *IEEE Trans. Power Electron.*, vol. 33, no. 1, pp. 226–239, Jan. 2018.
[9] N. R. Mehrabadi, R. Burgos, C. Roy, and D. Boroyevich, "Power electronics modeling and design: Using parametric and model-form uncertainty quantification to assess predictive accuracy of power converter models," *IEEE Power Electron. Mag.*, vol. 4, no. 4, pp. 44–52, Dec. 2017.
[10] R. Mehrabadi and Niloofar, "Power electronics design methodologies with parametric and model-form uncertainty quantification," Ph.D. dissertation, Virginia Tech, Blacksburg, VA, USA, 2018.
[11] M. Köksalan, J. Wallenius, and S. Zionts, "An early history of multiple criteria decision making," *J. Multi-Criteria Decis. Anal.*, vol. 20, no. 1/2, pp. 87–94, 2013.
[12] R. T. Marler and J. S. Arora, "The weighted sum method for multi-objective optimization: New insights," *Structural Multidisciplinary Optim.*, vol. 41, no. 6, pp. 853–862, 2010.
[13] N. Femia and G. Spagnuolo, "True worst-case circuit tolerance analysis using genetic algorithms and affine arithmetic," *IEEE Trans. Circuits Syst. I, Fundam. Theory Appl.*, vol. 47, no. 9, pp. 1285–1296, Sep. 2000.
[14] C. Z Mooney, *Monte Carlo Simulation*, vol. 116. Thousand Oaks, CA, USA: Sage Publications, 1997.
[15] S. Rangavajhala, C. Liang, and S. Mahadevan, "Design optimization under aleatory and epistemic uncertainties," in *Proc. 12th AIAA Aviation Technol. Integr. Oper. Conf. 14th AIAA/ISSMO Multidisciplinary Anal. Optim. Conf.*, 2012, Art. no. 5665.
[16] S. Nannapaneni, C. Liang, and S. Mahadevan, "Bayesian network approach to multidisciplinary, multi-objective design optimization under uncertainty," in *Proc. 18th AIAA/ISSMO Multidisciplinary Anal. Optim. Conf.*, 2017, Art. no. 3825.
[17] S. Sankararaman, and S. Mahadevan, "Model validation under epistemic uncertainty," *Rel. Eng. Syst. Saf.*, vol. 96, no. 9, pp. 1232–1241, 2011.
[18] R. H. Sues, and Y. Shin, "Applications of reliability-based design optimization," in *Engineering Design Reliability Handbook*. Boca Raton, FL, USA: CRC Press, 2004, pp. 845–868.
[19] S. Rangavajhala, and S. Mahadevan, "Design optimization for robustness in multiple performance functions," *Struct. Multidisciplinary Optim.*, vol. 47, no. 4, pp. 523–538, 2013.
[20] L. Empringham, L. de Lillo, P. W. Wheeler, and J. C. Clare, "Matrix converter protection for more electric aircraft applications," in *Proc. IEEE Ind. Electron. IECON-32nd Annu. Conf.*, 2006, pp. 2564–2568.
[21] P. W. Wheeler, J. C. Clare, A. Trentin, and S. Bozhko, "An overview of the more electrical aircraft," *Proc. Inst. Mech. Eng. Part G: J. Aerosp. Eng.*, vol. 227, no. 4, pp. 578–585, 2013.
[22] C. Gammeter, F. Krismer, and J. W. Kolar, "Weight and efficiency analysis of switched circuit topologies for modular power electronics in MEA," in *Proc. Ind. Electron. Soc., IECON-42nd Annu. Conf.*, 2016, pp. 3640–3647.
[23] G. Gong, M. L. Heldwein, U. Drofenik, J. Minibock, K. Mino, and J. W. Kolar, "Comparative evaluation of three-phase high-power-factor AC-DC converter concepts for application in future more electric aircraft," *IEEE Trans. Ind. Electron.* vol. 52, no. 3, pp. 727–737, Jun. 2005.
[24] R. M. Burkart, "Advanced modeling and multi-objective optimization of power electronic converter systems," Ph.D. dissertation, ETH Zurich, Zürich, Switzerland, 2016.
[25] R. Lai *et al.*, "A systematic topology evaluation methodology for high-density three-phase PWM AC-AC converters," *IEEE Trans. Power Electron.*, vol. 23, no. 6, pp. 2665–2680, Nov. 2008.
[26] D. G. Holmes and T. A. Lipo, *Pulse Width Modulation for Power Converters: Principles and Practice*, vol. 18. Hoboken, NJ, USA: Wiley, 2003.
[27] Y. Ren, M. Xu, J. Zhou, and F. C. Lee, "Analytical loss model of power MOSFET," *IEEE Trans. Power Electron.*, vol. 21, no. 2, pp. 310–319, Mar. 2006.
[28] T. Shimizu and S. Iyasu, "A practical iron loss calculation for AC filter inductors used in PWM inverters," *IEEE Trans. Ind. Electron.*, vol. 56, no. 7, pp. 2600–2609, Jul. 2009.
[29] K. Venkatachalam, C. R. Sullivan, T. Abdallah, and H. Tacca, "Accurate prediction of ferrite core loss with nonsinusoidal waveforms using only Steinmetz parameters," in *Proc. Comput. Power Electron. IEEE Workshop*, 2002, pp. 36–41.
[30] N. Rashidi, Q. Wang, R. Burgos, C. Roy, and D. Boroyevich, "Multi-objective design and optimization of power electronics converters with uncertainty quantification – Part II: Model-form uncertainty," *IEEE Trans. Power Electron.*, to be published, doi: 10.1109/TPEL.2020.3007227.

Niloofar Rashidi (Member, IEEE) received the B.S. degree in electrical engineering from the Amirkabir University of Technology, Tehran, Iran, in 2012, and the M.S. degree in electrical engineering, the M.A. degree in data analysis and applied statistics, and the Ph.D. degree in electrical engineering from the Virginia Polytechnic Institute and State University, Blacksburg, VA, USA, in 2014, 2017, and 2018, respectively.

From 2012 to 2018, she was a Research Assistant with the Center for Power Electronics Systems, Virginia Polytechnic Institute and State University. She is currently a Hardware Engineer with Apple, Inc., Cupertino, CA, USA. Her research interests include wide-bandgap semiconductor-based power conversion, modeling and design optimization of power electronics converters and systems, and design under uncertainty.

Dr. Rashidi is a member of the IEEE Power Electronics Society, IEEE Industry Applications Society, and ASME.

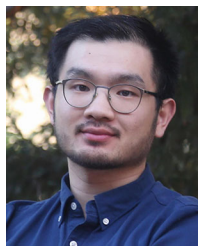

Qiong Wang (Member, IEEE) received the B.S. degree in electrical engineering from Tsinghua University, Beijing, China, in 2012, and the M.S. and Ph.D. degrees from Virginia Tech, Blacksburg, VA, USA, in 2015 and 2018, respectively.

In 2012, he joined the Center for Power Electronics Systems (CPES), Virginia Tech. He became a Research Scientist with CPES upon graduation and then joined Google as a Hardware Engineer. His research interests include power electronics circuit optimization, wide-bandgap devices applications, and multiphase multilevel power conversion.

Rolando Burgos (Member, IEEE) received the B.S. degree in electronics engineering, the Electronics Engineering Professional degree, and the M.S. and Ph.D. degrees in electrical engineering from the University of Concepción, Concepción, Chile, in 1995, 1997, 1999, and 2002, respectively.

In 2002, he joined as a Postdoctoral Fellow, with the Center for Power Electronics Systems (CPES), Virginia Tech, in Blacksburg, VA, USA, where he became a Research Scientist in 2003, and a Research Assistant Professor in 2005. In 2009, he joined ABB Corporate Research, Raleigh, NC, USA, where he was a Scientist from 2009 to 2010, and a Principal Scientist from 2010 to 2012. In 2010, he was appointed as an Adjunct Associate Professor with the Electrical and Computer Engineering Department, North Carolina State University at the Future Renewable Electric Energy Delivery and Management (FREEDM) Systems Center. In 2012, he returned to Virginia Tech as an Associate Professor with The Bradley Department of Electrical and Computer Engineering, where he has been Professor and member of the CPES Executive Board since 2019. His research interests include high power density wide-bandgap semiconductor-based power conversion—low voltage and medium voltage applications, packaging and integration, electromagnetic interference (EMI) and electromagnetic compatibility (EMC), multiphase multilevel power converters, modeling and control, grid power electronics systems, and the stability of ac and dc power systems.

Dr. Burgos is a member of the IEEE Power Electronics Society where he currently serves Chair of the Technical Committee on Power and Control Core Technologies. He also serves as an Associate Editor of the IEEE TRANSACTIONS ON POWER ELECTRONICS, and the IEEE JOURNAL OF EMERGING AND SELECTED TOPICS IN POWER ELECTRONICS. He is a member of the IEEE Industry Applications Society, the IEEE Industrial Electronics Society, and the IEEE Power and Energy Society.

Chris Roy received the undergraduate degree in mechanical engineering from Duke University, Durham, NC, USA, in 1992, the master's degree in aerospace engineering from Texas A&M University, College Station, TX, USA, in 1994, and the Doctorate degree in aerospace engineering from North Carolina State University, Raleigh, NC, USA, in 1998.

After spending five years as a Senior Member of the Technical Staff with Sandia National Laboratories, Albuquerque, New Mexico, he moved to academia and is currently a Full Professor with the Crofton Department of Aerospace and Ocean Engineering, Virginia Tech, Blacksburg, VA, USA. He has authored or coauthored more than 180 books, book chapters, journal articles, and conference papers in the areas of computational fluid dynamics, verification, validation, and uncertainty quantification. He is the co-author of the book *Verification and Validation in Scientific Computing* (Cambridge University Press, 2010).

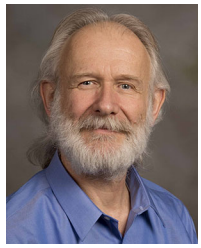

Dushan Boroyevich (Life Fellow, IEEE) received the Dipl.-Ing. degree from the University of Belgrade, Belgrade, Serbia, in 1976, the M.S. degree from the University of Novi Sad, Novi Sad, Serbia, in 1982, and the Ph.D. degree from Virginia Polytechnic Institute and State University (Virginia Tech), Blacksburg, VA, USA, in 1986.

From 1986 to 1990, he was an Assistant Professor and Director of the Power and Industrial Electronics Research Program with the Institute for Power and Electronic Engineering, University of Novi Sad. He then joined the Bradley Department of Electrical and Computer Engineering, Virginia Tech, as an Associate Professor. He is currently the University Distinguished Professor with the Department and Director of the Center for Power Electronics Systems. His research interests include electronic power distribution systems, multiphase power conversion, power electronics systems modeling and control, and integrated design of power converters.

Prof. Boroyevich was the President of the IEEE Power Electronics Society from 2011 to 2012. He is a member of the US National Academy of Engineering and is recipient of numerous awards, including the IEEE William E. Newell Power Electronics Technical Field Award and the European Power Electronics Association Outstanding Achievement Award.